Measurement of Cross-Magnetic-Field Heat Transport in a Pure Ion Plasma

E. M. Hollmann, F. Anderegg, and C. F. Driscoll

Physics Department and Institute for Pure and Applied Physical Sciences, University of California at San Diego,
La Jolla, California 92093
(Received 11 February 1999)

Cross-magnetic-field heat transport in a quiescent pure ion plasma is found to be diffusive and to be dominated by long-range collisions with impact parameters up to a Debye length. The measured thermal diffusivity χ agrees within a factor of 2 with the long-range prediction $\chi_L = 0.49 n \bar{v} b^2 \lambda_D^2$ over a range of 10^3 in temperature, 50 in density, and 4 in magnetic field. This thermal diffusivity is independent of magnetic field strength, and is observed to be up to 100 times larger than the classical diffusivity. These long-range collisions are typically dominant in unneutralized plasmas, and may also contribute to electron heat transport in neutral plasmas. [S0031-9007(99)09328-X]

PACS numbers: 52.25.Fi, 52.20.Hv, 52.25.Wz

Cross-magnetic-field heat transport is important for understanding magnetic fusion plasmas [1], astrophysical objects [2], plasma processing [3], and basic plasma physics [4]. "Collisional" transport is driven by the fluctuating fields from thermal motions of individual particles, whereas "turbulent" transport is driven by nonthermal fluctuations such as unstable waves or broadband turbulence. Plasmas with a single sign of charge are used for a wide range of basic plasma physics and atomic physics experiments [5]. These plasmas can be confined in a near-thermal equilibrium state where transport is dominated by collisions, rather than by turbulence; here we measure collisional heat transport in a quiescent pure ion plasma.

Direct Coulomb collisions between particles can occur over distances up to a Debye shielding length λ_D, but the character of the collision depends on the impact parameter ρ compared to the cyclotron radius r_c. Short-range (velocity-scattering) collisions (with $\rho < r_c$) cause perpendicular-to-parallel temperature equipartition and give "classical" heat transport. In contrast, long-range collisions (with $r_c < \rho < \lambda_D$) cause *no* perpendicular-to-parallel equipartition but give a heat transport which can be much larger than classical. These long-range collisions occur only in plasmas with $\lambda_D > r_c$.

Classical transport theory analyzes collisions with $\rho \lesssim r_c$. These collisions cause scattering between the perpendicular and parallel velocities and thus drive the perpendicular and parallel velocity distributions toward a Maxwellian with a single temperature T. For ion-ion collisions, the (momentum transfer) collision rate [6] is

$$\nu_{ii} = \frac{16}{15} \sqrt{\pi}\, n \bar{v} b^2 \ln\left(\frac{r_c}{b}\right)$$
$$\approx (1.0\ \text{s}^{-1}) T^{-3/2} n_7 [1 + 0.08 \ln(T^{3/2} B^{-1})], \quad (1)$$

where $b \equiv e^2/T$ is the distance of closest approach. Here, the numerical values are appropriate to $^{24}\text{Mg}^+$ ions, with density $n_7 \equiv n/10^7\ \text{cm}^{-3}$, magnetic field B in tesla, and temperature T in eV. The Coulomb logarithm reflects the ordering $r_c < \lambda_D$ appropriate to pure

ion plasmas, where $r_c \equiv \bar{v}/\Omega_c \approx (0.5\ \text{mm}) T^{1/2} B^{-1}$ and $\lambda_D \equiv [T/4\pi e^2 n]^{1/2} \approx (2.4\ \text{mm}) T^{1/2} n_7^{-1/2}$.

Direct measurements of the equipartition rate $\nu_{\perp\parallel} = \frac{1}{2}\nu_{ii}$ between perpendicular and parallel temperatures $T_\perp$ and $T_\parallel$ in pure ion plasmas [7] verify that these velocity-scattering collisions are correctly described by Eq. (1). These collisions also cause diffusion of particles, momentum, and heat. The classical thermal diffusivity χ_c is given [8] by

$$\chi_c = \nu_{ii} r_c^2$$
$$\approx (2.5 \times 10^{-3}\ \text{cm}^2\,\text{s}^{-1})$$
$$\times\, T^{-1/2} B^{-2} n_7 [1 + 0.08 \ln(T^{3/2} B^{-1})]. \quad (2)$$

This diffusivity is due to random radial steps of size r_c occurring at a rate ν_{ii}.

In this paper, we also consider the (larger) thermal diffusivity χ_L produced by long-range collisions with impact parameters $r_c < \rho < \lambda_D$. In these long-range collisions, the ions exchange parallel energies over radial distances ρ without change in the perpendicular velocities, so there is no contribution to the equipartition rate $\nu_{\perp\parallel}$. There is also a small $\mathbf{E} \times \mathbf{B}$ drift due to these collisions; this produces negligible heat transport but is important for particle and angular momentum transport [9]. The cross-field thermal diffusivity χ_L is calculated [10] to be

$$\chi_L = 0.49 n \bar{v} b^2 \lambda_D^2$$
$$\approx (1.1 \times 10^{-3}\ \text{cm}^2\,\text{s}^{-1}) T^{-1/2}. \quad (3)$$

These long-range collisions cause thermal diffusion which can be thought of as due to random radial steps of size λ_D occurring at a rate $n \bar{v} b^2$. Comparing Eqs. (2) and (3) suggests that the collisional heat transport will be dominated by long-range collisions in plasmas with $\lambda_D \gtrsim 7 r_c$. Single species plasmas are commonly in this regime due to the Brillouin density limit [11], and the electrons in some neutral plasmas are in this regime, i.e., $\lambda_D \gtrsim 7 r_{ce}$.

In addition to these direct Coulomb collisions, it is predicted that energy can be exchanged over distances

$\rho \gg \lambda_D$ by the thermal emission and absorption of lightly damped plasma waves [10]. These wave-mediated collisions are expected to dominate for thermal gradient length scales $L_T \gtrsim 100\lambda_D$ and may contribute to the large electron conductivity observed in tokamak plasmas [12]. However, this wave-mediated transport does not contribute to the present experiments, since $L_T < 100\lambda_D$. Also, the derivation of χ_L in Eq. (3) [10] presumes that $L_T > \lambda_D$, which is reasonably well satisfied in the experiments.

Thus, we expect to observe a diffusive cross-field heat flux Γ_q given by

$$\Gamma_q = -\frac{5}{2} n(\chi_L \nabla T_{\parallel} + \chi_c \nabla T) + \Gamma_{ND}, \qquad (4)$$

where $\nabla = \partial/\partial r$. Here, we have separately identified $T_{\parallel}$ to emphasize the unusual nature of χ_L, but for most of our experiments we can approximate $T_{\perp} \approx T_{\parallel} \equiv T$ to adequate accuracy. The term Γ_{ND} represents a possible heat flux due to nondiffusive effects such as waves or convection. We observe no consistent signature of these effects, so we take $\Gamma_{ND} = 0$.

Here, heat transport measurements are made on plasma columns consisting of uncorrelated magnesium ions, with temperatures $5 \times 10^{-4} < T < 0.5$ eV, densities $0.2 < n_7 < 10$, and magnetic fields $1 < B < 4$ T. The measurements show that the cross-magnetic-field heat flux in these plasmas is diffusive, with average thermal diffusivity $\chi \approx 1.7\chi_L$.

The experimental setup is shown in Fig. 1. Magnesium ions are created with a metal vacuum vapor arc and are trapped in a Penning-Malmberg trap [13] with uniform axial magnetic field B and end-confinement potentials $V_c = 200V$. Typically, $N_{tot} \approx 5 \times 10^8$ ions form a plasma column of length $L_p \approx 14$ cm and radius $R_p \approx 0.5$ cm inside conducting cylinders with radius $R_w = 2.86$ cm. These plasmas consist of about 70% Mg$^+$, with the remainder being mostly magnesium hydrides, MgH$_n^+$, formed

FIG. 1. Ion trap schematic showing manipulating beam and probe beam geometries.

when ions interact with the residual neutral background gas (H$_2$) at pressure $P \approx 4 \times 10^{-9}$ Torr.

The radial electric field due to the unneutralized ion charge causes the plasma column to $\mathbf{E} \times \mathbf{B}$ drift rotate at a (central) frequency of $f_E \equiv n(r = 0)ec/B \approx (14.4$ kHz$)n_7 B^{-1}$. Diamagnetic and centrifugal drifts are small, so the total fluid rotation frequency is $f_{rot} \approx f_E$. This rotation is rapid compared to the heat transport times discussed here, so our radial transport measurements are effectively azimuthally averaged. Individual thermal ions bounce axially at a rate $f_b \equiv \bar{v}/2L_p \approx (7.1$ kHz$)T^{1/2}(L_p/14$ cm$)^{-1}$, so we also assume the plasma to be uniform along the magnetic field lines.

These ion plasmas normally expand radially on a time scale of $\tau_m \approx 2000$ sec due to azimuthal asymmetries in confining fields. Here, however, the ions are held in near-thermal-equilibrium steady state for days or weeks through application of a weak "rotating wall" perturbation field [14]. The heating due to the slow plasma expansion (Joule heating) or due to the rotating wall drive is balanced by cooling from collisions with the background neutral gas, and the plasma typically relaxes to an equilibrium at $T \approx 0.05$ eV. In practice, the rotating drive is turned off during the heat transport experiments; however, we find that the results obtained for the thermal diffusivity are the same with the rotating wall on or off.

The plasma is diagnosed and heated or cooled using two continuous 280 nm lasers: a weak (≈ 10 μW) probe beam is used to nonperturbatively measure the plasma density, temperature, and fluid rotation velocity, and a stronger (≈ 1 mW) manipulating beam is used to vary the local plasma temperature. The manipulating beam is chopped, and the plasma temperature and density are measured using the probe beam during times when the manipulating beam is off. As indicated in Fig. 1, the probe beam can be aligned parallel or perpendicular to the magnetic field. Typically, the probe beam frequency is scanned through a $3^2S_{1/2} \rightarrow 3^2P_{3/2}$ cyclic transition of ^{24}Mg$^+$ at each radial position. The Doppler-broadened and -shifted laser induced fluorescence signal gives the ion velocity distribution $f(v)$.

From the measured ion distributions, $f_{\perp}(v_{\perp}, r, t)$ and $f_{\parallel}(v_{\parallel}, r, t)$, we obtain the local magnesium density $n_{Mg}(r)$, temperatures $T_{\perp}(r, t)$ and $T_{\parallel}(r, t)$, and fluid rotation velocity $v_{\theta}(r)$. In practice, the rapid temperature evolution is obtained from just the velocity distribution peaks, that is, $f_{\parallel}(0, r, t)$ or $f_{\perp}(v_{\theta}, r, t)$, since the ion density is constant with time. The total charge density $n(r)$ is calculated as that required to give $f_{rot}(r) = v_{\theta}(r)/2\pi r$. Typically, we find that $n_{Mg}(r)/n(r) \approx 0.7$ at all radii, so centrifugal mass separation [15] is negligible.

Heat transport experiments are performed by locally heating or cooling along the $r = 0$ axis of the plasma, thus creating an initial condition with a strong radial temperature gradient. This heating or cooling is obtained
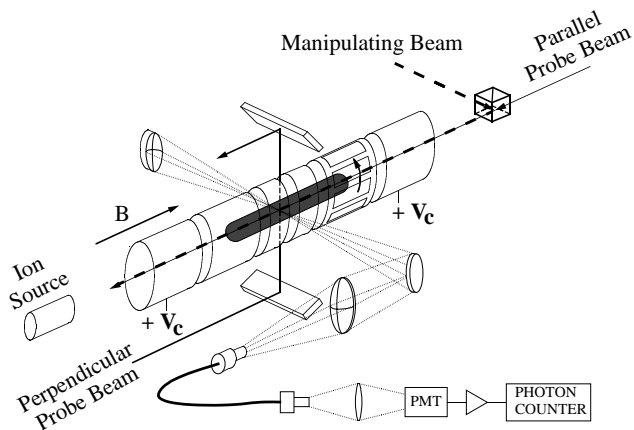
by detuning the parallel manipulating beam to the blue or red side of the cyclic transition. The perturbed $T_\parallel$ couples locally to $T_\perp$ in a time $\nu_{\perp\parallel}^{-1}$ which is short compared to the radial transport times, so $T_\parallel \approx T_\perp = T$ is an adequate approximation for these experiments. The time evolution of the plasma temperature, $T(r,t)$, is then measured after the manipulating beam is blocked with a shutter.

Figure 2 shows a typical evolution of $T(r,t)$ in an ion plasma with steady-state density profile $n(r)$. At $t = 0$, the cooling beam is turned off, and the central plasma temperature is observed to rise from $T \approx 3 \times 10^{-3}$ eV at $t = 0$ toward the equilibrium temperature of $T \approx 0.05$ eV. For clarity, only $t = 0, 0.1,$ and 1 sec and the final equilibrium state $t \to \infty$ are shown; actually, the temperature evolution is measured with 100 time steps over $0 < t < 4$ sec for each radial position.

The temperature evolution of Fig. 2 results from a radial heat flux plus small external heating terms. The radial heat flux Γ_q is obtained from the measured change in local energy density, $\dot{q}(r,t) \equiv \frac{\partial}{\partial t}[\frac{3}{2}n(r)T(r,t)]$ as

$$\Gamma_q(r,t) \equiv -\frac{1}{r}\int_0^r r'\,dr'[\dot{q}(r',t) - \dot{q}_{\text{ext}}(r',t)], \quad (5)$$

where the weak external heating or cooling term $\dot{q}_{\text{ext}}$ is known from independent measurements described below.

In Fig. 3, we plot the measured radial heat flux Γ_q as a function of the temperature gradient ∇T obtained from the data of Fig. 2. We plot the heat flux measured at radii $r = 0.1, 0.15,$ and 0.2 cm, and at times $t = 0.1$ to 1.9 sec; these radii were chosen here because they have a strong gradient and strong signal, i.e., $\dot{q} \gg \dot{q}_{\text{ext}}$. It can be seen that the gradients and fluxes are largest at early times and decrease as the temperature profile relaxes toward equilibrium. Since both classical and long-range transport predict $\Gamma_q \propto \chi \nabla T \propto T^{-1/2}\nabla T$, the displayed Γ_q is divided by $T^{-1/2}$ to better illustrate the proportionality with ∇T. The dashed line in Fig. 3 is an unconstrained linear fit to the data. The small nonzero

intercept could represent a nondiffusive flux; but here it seems to be insignificant, arising from uncertainties in the data or imperfect corrections $\dot{q}_{\text{ext}}$. Thus, Fig. 3 demonstrates diffusive heat conduction.

We calculate the local thermal diffusivity χ for each data point of Fig. 3 using

$$\chi(n, B, T) = -\frac{2}{5n}\frac{\Gamma_q}{\nabla T}. \quad (6)$$

Values of $\chi(n, B, T)$ were obtained for different equilibrium plasmas covering a range of 50 in density, 10^3 in temperature, and 4 in magnetic field. In Fig. 4, we plot the measured χ as a function of temperature T. Here, we display a single averaged value of χ for each evolution such as Fig. 3. For example, the data of Fig. 3 give an average thermal diffusivity $\chi \simeq 1.3 \times 10^{-2}$ cm^2 s^{-1} for an average temperature $T \simeq 0.028$ eV. This averaging has little consequence since the range of n, T, and χ in a single evolution is small. The dashed curves in Fig. 4 show the predicted classical thermal diffusivities χ_c for the five densities and magnetic fields used. The solid line shows the predicted long-range thermal diffusivity χ_L, which depends only on temperature.

The measured thermal diffusivities are up to 100 times larger than the classical prediction and are independent of B and n. The $T^{-1/2}$ scaling is observed over three decades in T and extends into the low-temperature regime where $r_c \approx b$. A fit to Fig. 4 with $\chi \propto T^{-1/2}$ gives $\chi = [(1.93 \pm 1) \times 10^{-3}$ cm^2 s$^{-1}]T^{-1/2} = (0.84 \pm 0.5)n\overline{v}b^2\lambda_D^2$.

The small external heating correction, $\dot{q}_{\text{ext}}$, used in Eq.(5) is obtained by measuring the temperature evolution of a plasma which has been *uniformly* heated or cooled by a wide manipulating beam. In the absence of radial temperature variation, we expect $\Gamma_q \approx 0$, implying that

FIG. 2. Measured thermal diffusion starting from locally ($r = 0$) cooled initial condition.
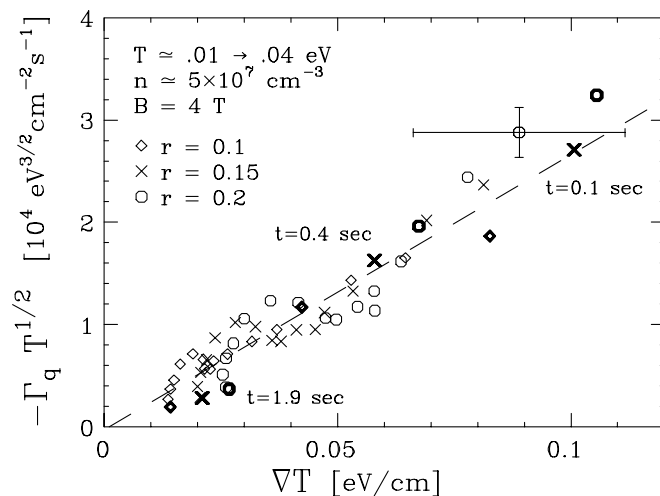
FIG. 3. Measured normalized radial heat flux vs temperature gradient for experiment shown in Fig. 2, demonstrating diffusive heat transport.
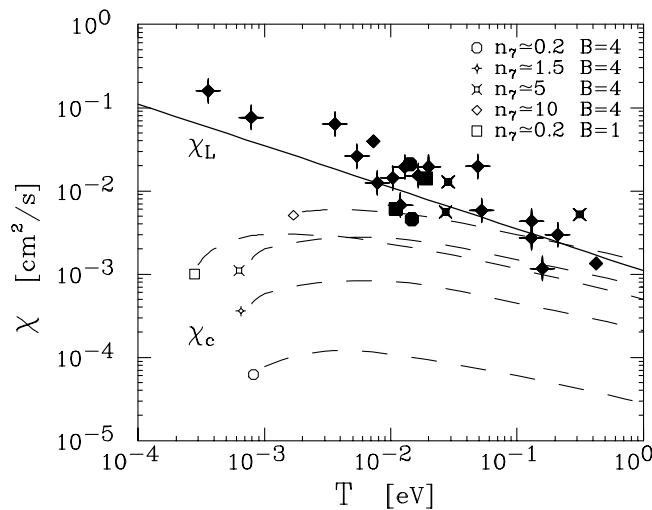
FIG. 4. The measured cross-magnetic-field thermal diffusivity χ plotted as a function of temperature T.

$\dot{q} \approx \dot{q}_{ext}$. This external heating was measured at $B = 4$ T for a range of parameters: $0.3 \times 10^{-9} < P < 4 \times 10^{-9}$ Torr, $1 < n_7 < 10$, and $10^{-3} < T < 2$ eV. The measurements are consistent with a model $\dot{q}_{ext} = \dot{q}_J + \dot{q}_N$ incorporating Joule heating, $\dot{q}_J$, plus heating or cooling due to ion-neutral collisions, $\dot{q}_N$. We obtain $\dot{q}_J(n, T, r)$ by measuring the expansion rate of the plasma with the rotating wall field turned off, and we estimate $\dot{q}_N(n, T)$ from the cross section of ions colliding with H_2 molecules. For the data presented here, the correction to χ is small, since $\dot{q}_{ext}/\dot{q} \approx 0.1$ in the regions with a large temperature gradient.

In summary, we have measured the cross-magnetic-field heat flux in a quiescent pure ion plasma. The heat flux is proportional to the thermal gradient ∇T and is apparently due to long-range collisions with impact parameter up to a Debye length. These long-range collisions cause heat fluxes which are independent of magnetic field strength: the observed thermal diffusivity scales as $\chi \propto n^0 B^0 T^{-1/2}$, as predicted for long-range collisions, whereas the thermal diffusivity resulting from classical, short-range collisions scales as $\chi_c \propto n B^{-2} T^{-1/2}$. At high magnetic field and low densities, the classical prediction is more than 2 orders of magnitude too small to explain the observed heat fluxes. This enhanced heat transport should occur in many nonneutral plasmas, where $\lambda_D > r_c$ is always satisfied, and may apply to the electron component of neutral plasmas which satisfy $\lambda_D \gtrsim 7 r_{ce}$.

[1] F. Wagner and U. Stroth, Plasma Phys. Control. Fusion **35**, 1321 (1993).

[2] S. M. Ichimaru, H. Iyetomi, and S. Tanaka, Phys. Rep. **149**, 93 (1987); B. D. G. Chandran and S. C. Cowley, Phys. Rev. Lett. **80**, 3077 (1998).

[3] M. Tuszewski, Phys. Plasmas **5**, 1198 (1998).

[4] A. T. Burke, J. E. Maggs, and G. J. Morales, Phys. Rev. Lett. **81**, 3659 (1998); D. D. Needelman and R. L. Stenzel, Phys. Rev. Lett. **58**, 1426 (1987).

[5] T. M. O'Neil, in *Non-neutral Plasma Physics,* edited by Gerry M. Bunce, AIP Conf. Proc. No. 175 (AIP, New York, 1988), P. 1; J. N. Tan, J. J. Bollinger, and D. J. Wineland, IEEE Trans. Instrum. Meas. **44**, 144 (1995).

[6] T. M. O'Neil and C. F. Driscoll, Phys. Fluids **22**, 266 (1979).

[7] F. Anderegg, X.-P. Huang, C. F. Driscoll, E. M. Hollmann, T. M. O'Neil, and D. H. E. Dubin, Phys. Rev. Lett. **78**, 2128 (1997); B. R. Beck, J. Fajans, and J. H. Malmberg, Phys. Rev. Lett. **68**, 317 (1992).

[8] M. N. Rosenbluth and A. N. Kaufmann, Phys. Rev. **109**, 1 (1958).

[9] D. H. Dubin, Phys. Plasmas **5**, 1688 (1998).

[10] D. H. E. Dubin and T. M. O'Neil, Phys. Rev. Lett. **78**, 3868 (1997).

[11] L. Brillouin, Phys. Rev. **67**, 260 (1945); R. C. Davidson, *Physics of Nonneutral Plasmas* (Addison-Wesley, Redwood City, CA, 1989), p. 42.

[12] M. N. Rosenbluth and C. S. Liu, Phys. Fluids **19**, 815 (1976); A. A. Ware, Phys. Fluids B **5**, 2769 (1993).

[13] F. Anderegg, X.-P. Huang, E. Sarid, and C. F. Driscoll, Rev. Sci. Instrum. **68**, 2367 (1997).

[14] X.-P. Huang, F. Anderegg, E. M. Hollmann, C. F. Driscoll, and T. M. O'Neil, Phys. Rev. Lett. **78**, 875 (1997); F. Anderegg, E. M. Hollmann, and C. F. Driscoll, Phys. Rev. Lett. **81**, 4875 (1998).

[15] T. M. O'Neil, Phys. Plasmas **24**, 1447 (1981).